International Journal of Chemical, Materials and Biomolecular Sciences
ISSN: 2415-6620
Vol:8, No:7, 2014

RBF Modelling and Optimization Control for Semi-Batch Reactors

Magdi M. Nabi, Ding-Li Yu

***Abstract*—**This paper presents a neural network based model predictive control (MPC) strategy to control a strongly exothermic reaction with complicated nonlinear kinetics given by Chylla-Haase polymerization reactor that requires a very precise temperature control to maintain product uniformity. In the benchmark scenario, the operation of the reactor must be guaranteed under various disturbing influences, e.g., changing ambient temperatures or impurity of the monomer. Such a process usually controlled by conventional cascade control, it provides a robust operation, but often lacks accuracy concerning the required strict temperature tolerances. The predictive control strategy based on the RBF neural model is applied to solve this problem to achieve set-point tracking of the reactor temperature against disturbances. The result shows that the RBF based model predictive control gives reliable result in the presence of some disturbances and keeps the reactor temperature within a tight tolerance range around the desired reaction temperature.

***Keywords*—**Chylla-Haase reactor, RBF neural network modelling, model predictive control.

I. Introduction

BATCH and semi-batch reactors are widely used in the production of fine chemicals, pharmaceuticals, specialties and other high value products because of their flexibility in operation mode. This type of reactor is industrially important and particularly well-matched for the production of polymers of varying grades, whose quality is measured in terms of strength, process ability, etc. [1]-[3]. The control task in this work is to keep the temperature constant throughout the production. Thereby, the step-like monomer feed poses a significant demand on the control in order to keep the reactor temperature within a specified tolerance interval, so it's necessary to improve control strategy of such a process in order to ensure that the end product will have acceptable quality. Polymerization reactors commonly controlled by a cascade controller, this method provides a robust operation, but lacks in control performance, efforts have been made to use advanced non-conventional control methods to develop and test alternative control schemes for improving the operational performance of exothermic batch processes.

In [2], [3]. The traditional proportional-integral (PI) cascade control is widely used in the semi-batch polymerization reactor because of the minimal requirement of process knowledge for its design. However, perfect control is unavailable because it fails to provide predictive control action to compensate for the effects of known disturbances. Although feed-forward control is used to improve the controller performance

In [4]. Reaction calorimetry for vapor-liquid (VL) systems and formulated in the framework of model predictive control (MPC) discussed possibilities for on-line optimization of semi-batch reaction systems through MPC in combination with state estimation.

Inverse dynamics modelling based neural networks proposed in [6]. The controller tries to mimic the inverse dynamics of the plant so that the plant is driven to the desired set-point.

A nonlinear adaptive temperature control proposed in [7]. This scheme promises disturbance rejection due to its ability to update parameters online.

Inverse neural network in hybrid scheme used to model and control the semi-batch polymerization process can be found in [8]. More robust advanced control were proposed in [9]-[10].

The structure of the RBFNN is described in the paper. In the simulation part, an RBFF network is trained using the Recursive Least Square method and used as the simulated process, then applying MPC, The main objectives of the predictive control strategy using RBF network is to estimate the future output of the plant and to minimize the cost function based on the error between the predicted output of the process and the reference trajectory.

The paper is organized as follows: In Section II process description of Chylla-Haase and the dynamic model is presented. Section III presents modelling of the system dynamics using RBF network and predictive model. MPC structure and simulation is given in Section IV. Finally the paper is concluded in Section V.

II. Chylla-Haase Polymerization Reactor

A. Process Description

The industrial polymerization process described by Chylla and Haase [1] consists of a stirred tank reactor with a cooling jacket and a coolant recirculation, a common strategy is shown in Fig. 1.

Magdi. M. Nabi and Ding-Li Yu are with the Control System Research Group, Liverpool John Moores University, United Kingdom (e-mail: M.M.Nabi@2010.ljmu.ac.uk,D.Yu@ljmu.ac.uk).

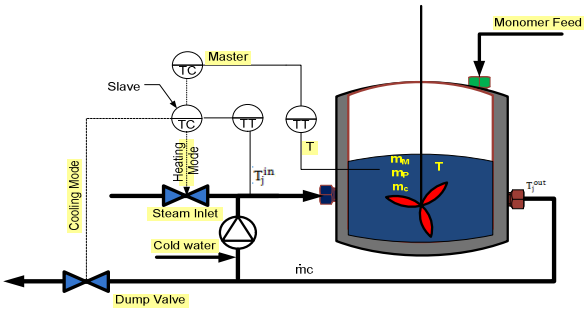

Fig. 1 Chylla-Haase reactor schematic

The temperature of the reactor is often ramped up from the ambient reactor charge conditions to a temperature where the reaction begins to take off. The heat released through the reaction must be removed by circulating cold water through the jacket, where both hot and cold jacket steam are available. When the jacket temperature controller output is between 0 and 50%, the valve is opened and cold water is inserted, and when the jacket controller output is between 50 and 100%, the valve is opened and steam is inserted [1], [2].

B. Reactor Dynamic Model

Simulink model of the reactor is developed using Matlab/Simulink, according to the mathematical model equation (1)-(5) below.

$$\frac{dm_M}{dt} = \dot{m}_M^{in} - R_p \tag{1}$$

$$\frac{\mathrm{dmp}}{\mathrm{dt}} = \mathrm{R_p} \tag{2}$$

$$\frac{dT}{dt} = \frac{1}{\sum_i mi\ \mathrm{Cp,i}}[\dot{m}_M^{in}\ \mathrm{C_{p,M}}(T_{Amb} - T) - UA(T - T_j) - (UA)_{loss}(T - T_{Amb}) + Q_{\mathrm{Re}a}] \qquad (i = M, P, W). \tag{3}$$

$$\frac{dT_j^{out}}{dt} = \frac{1}{m_c C_{P,c}}[\dot{m}_c\ \mathrm{C_{P,c}}(T_j^{in}(t-\theta_1) - T_j^{out}) + UA(T - T_j)] \tag{4}$$

$$\frac{dT_j^{in}}{dt} = \dot{T}_j^{out}(t-\theta_2) + \frac{T_j^{out}(t-\theta_2) - T_j^{in}}{\tau_P} + \frac{K_p(c)}{\tau_P} \tag{5}$$

First two equations (1) and (2) describe material balances for the monomer mass mM(t) and the polymer mass mP(t), (3), (4) and (5) define energy balance with the reactor temperature T(t), cooling jacket and the recirculation loop with the outlet and inlet temperatures $\mathrm{T_j^{in}}(t)$ and $\mathrm{T_j^{out}}(t)$ of the coolant C [2]. Additional variables and parameters are defined in Tables II-IV.

The heating/cooling function K_P is defined by (6) and is a function of the valve position c (t), [2]-[11]:

$$K_p(c) = \begin{cases} 0.8 \cdot 30^{-c/50}(T_{inlet} - T_j^{in}(t)), & C < 50\% \\ 0 & C = 50\% \\ 0.15 \cdot 30^{-c/50-2}(T_{steam} - T_j^{in}(t)), & C > 50\% \end{cases} \tag{6}$$

Various disturbances and uncertainties are specified in order to model the following practical problems with the control of polymerization reactors.

- The impurity factor $i \in [0.8, 1.2]$ in the polymerization rate RP is random and constant during one batch; it tries to model fluctuations in monomer kinetics caused by batch-to-batch variations in reactive impurities. The fouling factor $\frac{1}{hf}$ in theoverall heat transfer coefficient U increases with each batch andaccounts for the fact that during successive batches a polymer film builds up on the wall, resulting in a decrease of U [6], [7].
- The delay times θ1 and θ2 of the cooling jacket and the recirculation loop may vary by ±25% compared to the nominal values in Table III.
- The ambient temperature T_{amb} is different during summer and winter. This affects the temperature of as well as the initial conditions $T(0)$, $T_j^{in}(0)$, $T_j^{out}(0)$given by T_{amb}.
- Measurement noise is added to the temperature measurements with standard deviation σ(y) = 0.5.

Two different products data, A and B, are given in [1]-[3]. This work is restricted to product B only, and the following table shows scenarios considered for the robustness analysis.

TABLE I
CONSIDERED DISTURBANCES SCENARIO

Scenario	$i[-]$	$^1/_{hf}\ [m\text{^}2\ KkW^{-1}]$	$T_{amb}[K]$
1	0.8	0	280.382
2	1.2	0.704	280.382
3	0.8	0	305.382
4	1.2	0.704	305.382

III. NEURAL MODEL BASED- PREDICTIVE CONTROL ALGORITHM

A. Predictive Model

Considering that the two inputs and signal output nonlinear process can be given as a discrete time model:

$$y(k+1) = f[y(k-1), ..., y(k-n), u1(k-m), u2(k-l)] \tag{7}$$

where $y(k+1)$ is the process output,$u1(k-m)$ is the past input at time instant, $u2(k-l)$ is the second input (disturbance) and f is the unknown non-linear function, n, m, l respectively are the orders of the output and input.

A wide range multi-step direct predictive value can be obtained according to the past output and input together with the future input Assuming the time horizon is ,N , then

$$y(k+i) = f[y(k+i-n),..., y(k+i-1),..., u1(k+i-n),..., u1(k+i-1),..., u2(k+i-l),..., u2(k+i-1)] \tag{8}$$

where$i$ = 1, 2,…,N

B. RBF Neural Network Model and Training Algorithm

The neural network (RBF) can be used to construct the above predictive model (8), consisting from three layers, as

shown in Fig. 2, the first layer is the input, the second is the hidden layer, and the third is the output layer whose output is

$$\hat{y} = \sum_{j=1}^{nh} \phi_j(t) \bullet W_{ji} \qquad i = 1,.....q \tag{9}$$

where, ϕ_j defined by (10), w are the output layer weights and q is the number of outputs. The method that used in this work to calculate the Euclidean distance between the centre and the network input vector X_1 is Gaussian basis function [12], [13]. As shown in (10):

$$\phi_j(t) = \exp\left(-\frac{\left\|X_1(t) - c_j(t)\right\|^2}{\sigma_j^2}\right), \qquad j = 1,..,nh \tag{10}$$

where, σ_j is a positive scalar called width and c_j is the number of centers identified by K-means clustering data using Matlab tool box.

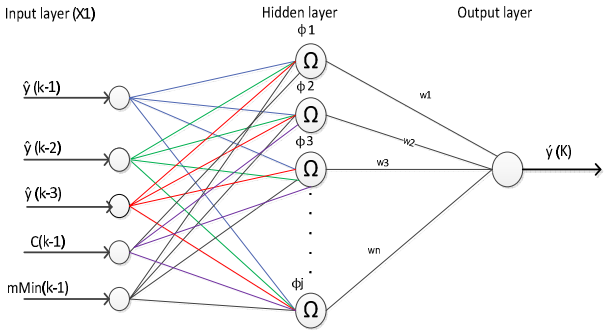

Fig. 2 Structure of RBFNN reactor model

Identifying of the non-linear model off-line before the controller is put into use, then adjusting the error between the estimated value and the practical output on-line, modifying the weight to optimize the model structure. Many optimization techniques can be used, recursive least square algorithm is used here to accomplish this task and can be summarized as [12], [13]:

$$y_p(k) = y(k) - w(k-1) * \phi(k) \tag{11}$$

$$g_z(k) = \frac{p_z(k-1)\,\phi(k)}{\mu + \phi'(k)\; p_z(k-1)\,\phi(k)} \tag{12}$$

$$p_z(k) = \mu^{-1}[p_z(k-1) - g_z(k)\,\phi'(k)\; p_z(k-1)] \tag{13}$$

$$w(k) = w(k-1) + g_z(k)\; y_p(k) \tag{14}$$

where, $w(k)$ and $\phi(k)$ represent the RBF network weights and activation function output respectively, $y(k)$is the process output vector, p_z and g_z are middle terms, μ is called the forgetting factor ranging from 0 to 1 and chosen to be 1 for offline training. The parameters g_z, w, and p_z are updated orderly for each sample with the change in the activation function output ϕ(k).

In order to guarantee the generalization of the trained neural network and confirm the acceptance of the network performance over a wide range of process operating conditions, the network needs to be trained with data which covers the entire range of possible network inputs. The training proceeded by randomly selecting values for the input variables within the specified ranges at a sampling time of 4 sec. The 3000 samples are used for training and a different 3000 samples are used for testing as shown in Figs. 3, 4. It presents a good match between reactor output and RBFNN output with error of 0.0197K based on mean absolute error (MAE), (15) which is used to evaluate the modelling and control performance in this work.

$$\text{MAE} = \frac{1}{N}\sum_{k=1}^{N} \left|\hat{y}(k) - y(k)\right| = \frac{1}{N}\sum_{k=1}^{N} \left|e(k)\right| \tag{15}$$

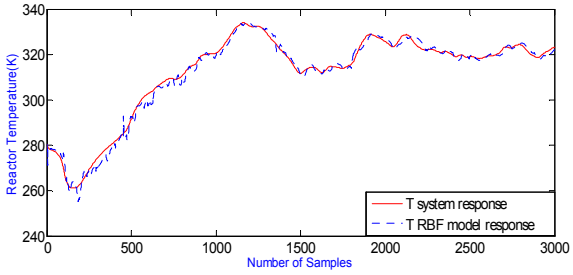

Fig. 3 Modelling result of the RBF model MAE = 0.0197

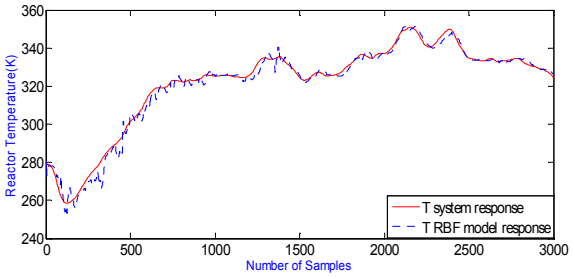

Fig. 4 Modelling result of the RBF model MAE= 0.612

IV. MPC Structure and Simulation

A. Control System Structure

The NN-MPC structure for the reactor is shown in Fig. 5. The obtained RBF neural network model in previous section is used to predict the reactor output for N_2 steps ahead. The nonlinear optimizer minimizes the errors between the set-point and the predicted output, as well as the increment of the optimized control variable by using the cost function (16).

$$J = \sum_{i=t+N_1}^{t+N_2} [y_{set}(i) - \hat{y}(i)]^2 + \lambda \sum_{i=t}^{t+N_u} [C(i) - C(i-1)]^2 \tag{16}$$

$$C\min \le C \le C\max \qquad (16.1)$$

This minimization is subject to constraint (16.1) valve position. Here, N_1, N_2 defines the prediction horizon, λ is a control weighting factor, N_u control horizon, y_{set} is the set-point, C is the valve position . The remaining main problem of MPC is to solve the nonlinear optimization problem in each sample period, calculate a series of optimal $C(t), C(t+1), \ldots, C(t+N_u\text{-}1)$ from which the neural network model generates output to minimize J [9]-[13].

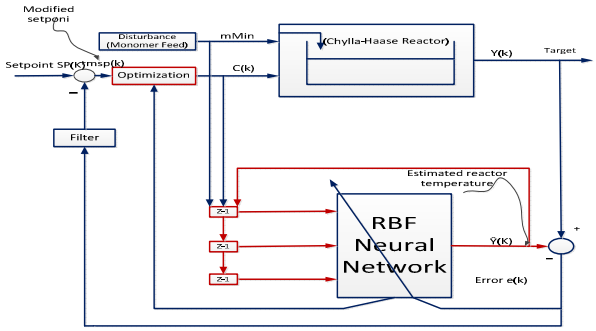

Fig. 5 The scheme of neural network based predictive control

B. Control Parameter Tuning

The prediction horizons were set at their best values of N_1=1, N_2=50, the control horizon N_u is set to be zero. For the minimization of the cost function, the Matlab's Optimal Toolbox functions (Fmincon) was used, which allow dealing with either unconstrained or constrained optimization problems. Fmincon allows imposing constraints with respect to the value of the control input such as upper or lower bounds. After attempting different values, the control weight is $\lambda = 0.025$, data sampling interval is 4 seconds.

C. Simulation Results

In this paper the simulation adopts a nonlinear semi-batch polymerization reactor. The performance of the RBFNN in tracking with different disturbances, impurity factor and fouling factor with four scenarios, first and fifth batch in summer ($T_{amb} = 305.382\ K$), first and fifth batch in winter ($T_{amb} = 280.382\ K$)

A result of the RBF based MPC strategy is shown in Figs. 6 (a)-(c). Significant improvement can be seen for the reactor temperature in Fig. 6 (a) using RBFNN based MPC even in the fifth batch which has big disturbance effect on the temperature the RBFNN still can maintain the temperature within the tolerance range which is ($\pm$0.6K) from the set point.

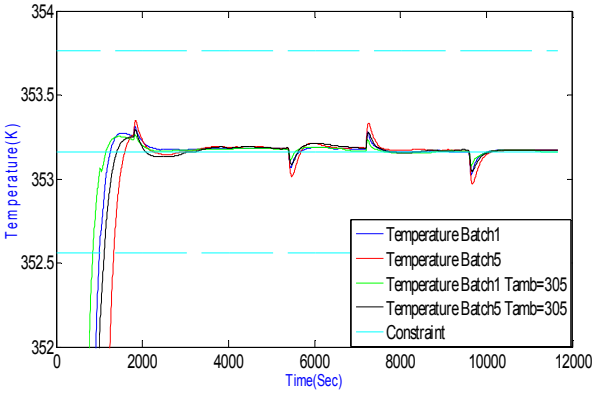

Fig. 6 (a) Reactor Temperature based on MPC

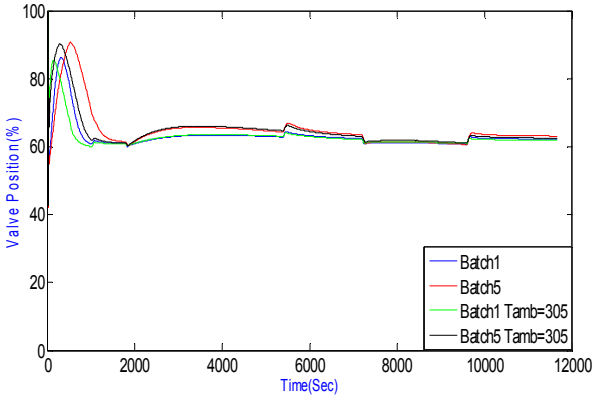

Fig. 6 (b) Valve Position based on MPC

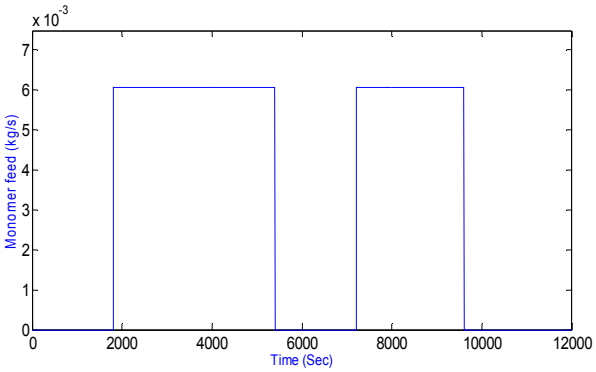

Fig. 6 (c) Monomer feed rate

The mean square error used here to evaluate the control performance and shows the strong capability of disturbance rejection of adaptive MPC based on RBF model (MSE= 0.0682 for the first bath and MSE= 1.0181) for the fifth batch.

V. Conclusion

This paper has discussed the RBF neural network based MPC for polymerization reactor given by Chylla-Haase. The RBF used to model a nonlinear model and to predict the future output. The simulation shows that the trained neural network was capable of capturing dynamics with a very small

performance tolerance indicating its high prediction accuracy. Implementation of the NNMPC controller was able to force process output to follow the target within its tolerance against influence of monomer feed, disturbances and uncertainties.

Further work will include control ability for more uncertainties and disturbances, and by the fact the monomer feed rate is constant which leads to long duration of the batch run, another optimization scheme is needed in order to make the monomer feed vary to reduce batch run.

TABLE II
EMPIRICAL RELATIONS FOR THE POLYMERIZATION RATE R_p, THE JACKET HEAT TRANSFER AREA A, AND THE OVERALL HEAT TRANSFER COEFFICIENT U

$R_P = iKm_M$	i =Impurity factor
$K = K_0 \exp(-\frac{E}{RT}) \cdot (K_1\mu)^{K_2}$	Kinetic constant
$\mu = c_0 \exp(c_1 f) \cdot 10^{c_2(a_0/T - c_3)}$	Batch viscosity
$f = m_p / (m_M + m_p + m_c)$	Mass function
$A = (\frac{m_M}{\rho_M} + \frac{m_P}{\rho_P} + \frac{m_W}{\rho_W})\frac{P}{B_1} + B_2$	Jacket heat transfer area
$U = \frac{1}{h^{-1} + h_f^{-1}}$ with $h = d_0 \exp(d_1\mu_{wall})$	Heat transfer coefficient

TABLE III
PARAMETER VALUES OF CHYLLA-HAASE REACTOR

Symbol	Unit	Values of Polymer B
$m_{M,0}$	kg	0
$m_{p,0}$	kg	11.010
m_w	kg	41.2825
ρ_M	kgm^{-3}	900
ρ_p	kgm^{-3}	1040
ρ_w	kgm^{-3}	1000
$C_{p,M}$	$kJkg^{-1}k^{-1}$	1.675
$C_{p,P}$	$kJkg^{-1}k^{-1}$	3.140
$C_{p,W}$	$kJkg^{-1}k^{-1}$	4.187
MW_M	$kgkmol^{-1}$	106.0
m_c	kg	42.996
$\dot{m}_c$	kg/s	0.9412
$C_{p,C}$	$kJkg^{-1}k^{-1}$	4.187
K_0	S^{-1}	20
K_1	$m\,s\,kg^{-1}$	1000
K_2		0.4
E	$kJkmol^{-1}$	29560.89
c_0	$kgm^{-1}S^{-1}$	3.2×10^{-5}
c_1		19.1
c_2		2.3
c_3		1.563
a_0	k	555.556
ΔH_p	$kJkmol^{-1}$	65593.2
d_0	$kW\,m^{-2}k^{-1}$	0.814
d_1	$m\,s\,kg^{-1}$	-5.13
$m_M^{in,max}$	kg/s	6.048×10^{-3}
$[t_{M,0}^{in}, t_{M,1}^{in}]$	min	[30,90]
$[t_{M,2}^{in}, t_{M,3}^{in}]$	min	[120,160]
T^{set}	K	353.160

TABLE IV
NOTATION OF THE CHYLLA-HAASE REACTOR

$\dot{m}_M^{in}$	Monomer feed rate [kg/s]
$Q_{Reaa} = -\Delta H \bullet R_P$	Reaction heat [kw]
R_P	Rate of polymerization [kg/s]
$-\Delta H$	Reaction enthalpy [kj/kg]
U	Overall heat transfer coefficient [kw/mk]
A	Jacket heat transfer area [m2]
$(UA)_{loss}$	Heat loss coefficient [kw/k]

REFERENCES

[1] R. W. Chylla and D. R. Haase, "Temperature control of semibatch polymerization reactors," *Computer Chem. Engng,* vol. 17, pp. 257-264, 1993.

[2] K. Graichen, V. Hagenmeyer, and M. Zeitz, "Adaptive Feedforward Control with Parameter Estimation for the Chylla-Haase Polymerization Reactor," in *Decision and Control, 2005 and 2005 European Control Conference. CDC-ECC '05. 44th IEEE Conference on*, 2005, pp. 3049-3054.

[3] K. Graichen, V. Hagenmeyer, and M. Zeitz, "Feedforward control with online parameter estimation applied to the Chylla–Haase reactor benchmark," *Journal of Process Control,* vol. 16, pp. 733-745, 2006.

[4] A. Helbig, O. Abel, and W. Marquardt, "Model predictive control for online optimization of semi-batch reactors," in *American Control Conference, 1998. Proceedings of the 1998*, 1998, pp. 1695-1699 vol.3.

[5] A. Helbig, O. Abel, A. M'hamdi, and W. Marquardt, "Analysis and Nonlinear Model Predictive Control of the Chylla-Naase Benchmark Problem," presented at the Proc.UKACC Int. Conf.control, 1996.

[6] A. Bhat and R. N. Banavar, "The Chylla-Haase Problem: A Neural Network Controller," presented at the International Conference on Control Applications, Trieste, Italy, 1998.

[7] T. Clarke-Pringle and J. F. MacGregor, "Nonlinear adaptive temperature control of multi-product, semi-batch polymerization reactors," *Computers & Chemical Engineering,* vol. 21, pp. 1395-1409, // 1997.

[8] C. W. Ng and M. A. Hussain, "Hybrid neural network—prior knowledge model in temperature control of a semi-batchpolymerization process," *Chemical Engineering and Processing: Process Intensification,* vol. 43, pp. 559-570, 2004.

[9] S. Lucia, T. Finkler, D. Basak, and S. Engell, "A new Robust NMPC Scheme and its Application to a Semi-batch Reactor Example," presented at the 8th IFAC Symposium on Advanced Control of Chemical Processes, The International Federation of Automatic Control, Furama Riverfront, Singapore,, 2012.

[10] T. F. Finkler, S. Lucia, M. B. Dogru, and S. Engell, "Simple Control Scheme for Batch Time Minimization of Exothermic Semibatch Polymerizations," *Ind. Eng. Chem.,* vol. 17, pp. 5906–5920, 2013.

[11] M.-A. Beyer, W. Grote, and G. Reinig, "Adaptive exact linearization control of batch polymerization reactors using a Sigma-Point Kalman Filter," *Journal of Process Control,* vol. 18, pp. 663-675, 2008.

[12] M. Pottmann and D. E. Seborg, "A nonlinear Predictive Control Strategy Based on Radial Basis Function Models," *Computer Chem. Engng,* vol. 21, pp. 965-980, 1997.

[13] D. L. Yu, J. B. Gomm, and D. Williams, "Online predictive control of a chemical process using neural network models," presented at the Proc.14th IFAC Congress,, Beijing, 1999.